WAVE PROPAGATION OVER A STEEP BATHYMETRIC SLOPE: INFLUENCE OF THE BED POROSITY ON THE WAVE PHASE MATCHING

Olivier David De Drézigué[1], Damien Sous[1] and Vincent Rey[1]

Abstract

In the present study, the wave propagation over a rectangular porous bar was investigated. The measurements of the reflection coefficient versus frequency for both porous and impervious bars were first compared to numerical results based on linear theories for gravity waves. The results have shown that the interference process is weakly influenced by the porosity of the bar and by the presence of impervious vertical boundaries at both sides of the bar. On the contrary, the bar steps and their characteristics have a local significant influence in terms of wave celerity and horizontal velocity components.

Key words: Laboratory experiments, gravity waves, rectangular bar, porous obstacle, wave reflection, evanescent modes, wave crest celerity

1. Introduction

Wave propagation over varying topography modeling is of great interest for both oceanographic and engineering purposes. It is well known that, in the presence of a bottom with depth discontinuities, not only propagating but also evanescent modes fully participate to the wave evolution. Their presence was demonstrated experimentally for a rectangular obstacle through the surface elevation down-wave the bar (Rey et al, 1992). For smoothly varying topography, its role in the interference processing was demonstrated for doubly sinusoidal bathymetry through comparison between calculated and measured reflection coefficient (Guazzelli et al, 1992). Indeed, the evanescent terms modify the wave phase evolution what is observed on the wave reflection maxima and minima as a function of the frequency, behavior enhanced by the interference process for finite length obstacles (see e.g. Rey, 1992).

Wave induced motion within a porous bed modifies the dispersion relation (Liu and Dalrymple, 1984) that leads to wave damping through porous beds or structures dissipative effects (Yu and Chwang, 1994). The two solutions of the relation dispersion corresponding to the propagating modes (incident and reflected) then include a damping term.

The purpose of the present study was the analysis of both the wave reflection and the wave behavior above an either impermeable or porous rectangular obstacle in order to better characterize the porous bed. Experiments have been carried out in a wave tank for regular wave of various period and amplitudes. Results are compared to the classical linear wave models including non propagating modes based on integral matching conditions at depth discontinuities (see e.g Rey, 1992 for the impermeable beds; Yu and Chwang, 1994 for porous beds).

[1] Université du Sud Toulon-Var, MIO, 83957, La Garde cedex; CNRS/INSU, MIO UMR 7294; IRD, MIO UMR 235, France

2. Experimental set-up

Experiments have been carried out in a wave tank of water depth h=0.30 m and useful length 10 m. The X-axis corresponds to the incoming wave direction of propagation, the Z-axis is vertical oriented upwards, Z=0 at the still water level. The location X=0 corresponds to the up-wave vertical boundary of the bar. At one end, a flap paddle allowed the generation of regular waves, at the other end, a parabolic beach allowed the incoming wave dissipation to prevent any beach reflection. The rectangular obstacle is 3m long and 0.15m high (see Fig. 1). The water depth above the obstacle is d=0.15m. The studied rectangular bar was either porous or solid. For the porous case, additional experiments have been carried out with impervious vertical boundaries. The porous media was made of gravels of mean diameter 7 mm. The mean porosity was of about 0.3. A series of synchronized wave gauges was used for the measurement of both wave reflection and transmission and beach reflection by use of the classical three wave gauge method. A pair of synchronized gauges could be moved along the wave tank for the measurement of the wave amplitude and celerity up-wave, over and down-wave the bar. Acoustic velocimeters (Vectrino manufactured by Nortek) were used for the high frequency 3D velocity measurement in the near vicinity of the porous bed, see Fig. 1.

In a first series of experiments, both wave reflection and phase evolution above the bar were calculated for two wave maker amplitudes (hereafter called series 1a and series 1b). In a second series of experiments, only the porous bar case was considered, but with either impervious or porous vertical boundaries. During this later series, both wave reflection versus frequency and wave amplitude effect at given frequency were investigated.

Figure 1. Pictures of the experimental setup

3. Analytical models and numerical procedures

Assuming linear waves, a general expression of the velocity potential is defined for each sub-domain of constant depth. The solution forced by an incoming wave of frequency $\omega=2\pi f$ is obtained by use of the classical integral matching method of both pressure and fluid velocities at vertical boundaries between sub-domains (see e.g Rey, 1992; Yu and Chwang, 1994). In the present case, the flow is

divided into three domains. Within domains 1 (X<0) and 3 (X>L=3m), respectively on both sides of the bar, the general form of the velocity potential is the sum of two propagating modes in the X-axis direction and an infinity of evanescent modes. For each domain j=1, 3, the general expression of the velocity potential can be written :

$$\phi_j(x,z,t) = e^{i(\omega t)}\left[\sum_{n=0}^{\infty} A_{j,n}{}^{\pm} e^{\pm(k_{j,n}x)}\psi_{j,n}\right] \tag{1}$$

with $\psi_{j,n} = \cos(k_{j,n}(z+h_j))$. The wavenumbers $k_{j,0} = \pm ik_j$ correspond to the two propagating waves, wavenumbers $\pm k_{j,n}$ correspond to the evanescent modes, of infinite number. Their values are given by the "dispersion relation":

$$\frac{\omega^2}{g} = -k_{j,n}\tan(k_{j,n}h_j) \tag{2}$$

For the case of the rectangular bar (case 1), the general form of the potential, defined above the bar (0>z>-d) and the relation dispersion are given respectively by (1) and (2), with j=2 and $\psi_{2,n} = \cos(k_{2,n}(z+d))$.

For the case of a superimposition of two porous layers, the general expression of the potential for the domain 2 (0<x<L) is given by (Yu and Chwang, 1994):

$$\phi_{2\sup}(x,z,t) = e^{i(\omega t)}\left[\sum_{n=0}^{\infty} A_{2,n}{}^{\pm} e^{\pm(k_{2,n}x)}\cos(k_{2,n}(h_2-d))\left(\frac{-igk_{2,n}}{\omega^2 Z_1}\cos(k_{2,n}z)+\sin(k_{2,n}z)\right)\right] \tag{3}$$

for 0>z>-d and by:

$$\phi_{2\inf}(x,z,t) = \alpha e^{i(\omega t)}\left[\sum_{n=0}^{\infty} A_{2,n}{}^{\pm} e^{\pm(k_{2,n}x)}\cos(k_{2,n}(h_2-d))\left(\frac{-igk_{2,n}}{\omega^2 Z_1}\cos(k_{2,n}z)+\sin(k_{2,n}z)\right)\right] \tag{4}$$

for $-d>z>-h_2$.

where $Z_m=f_m+iS_m$, m=1 (upper layer), 2 (bottom layer) is the dimensionless impedance of the porous medium, $\alpha=Z_1/Z_2$. The real part f_m of the impedance reflects the medium resistance while the imaginary part, $S_m=1+C_m(1-\gamma_m/\gamma_m)$ is the medium reactance. C_m is coefficient representing the inertial effect of the medium to the flow, γ_m is the porosity of the layer. The dispersion relationship is given by:

$$iZ_1\frac{\omega^2}{g} = -k_{2,n}\frac{\tan\beta k_{2,n}h_2 + \frac{\alpha}{\delta}\tan(1-\beta)k_{2,n}h_2}{1-\frac{\alpha}{\delta}\tan\beta k_{2,n}h_2\tan(1-\beta)k_{2,n}h_2} \tag{5}$$

where $\beta=d/h_2$ and $\delta=\gamma_1/\gamma_2$. In the present case, the upper layer is a free fluid and $Z_1=i$.

The solution is forced by an incoming wave of frequency $\omega=2\pi f$ of amplitude:

$$a^{-}_{1,0} = A^{-}_{1,0} k_1 \sinh k_1 h_1 / \omega$$

The coefficient $A^{+}_{3,0}=0$ for a perfect absorbing beach. The other coefficients are calculated through a classical integral matching method by using the orthogonal function $\psi_{j,n}$ for both the pressure and fluid velocities continuities at vertical boundaries between sub-domains. The evanescent modes are truncated at an order n=P.

The conditions are as follows:

Case 1:

$$\begin{cases} \int_{-d}^{0} \psi_{1,n}\phi_1 dz = \int_{-d}^{0} \psi_{1,n}\phi_2 dz \\ \int_{-h_1}^{0} \psi_{1,n}\partial\phi_1/\partial x dz = \int_{-d}^{0} \psi_{1,n}\partial\phi_2/\partial x dz \end{cases}, \quad \text{for x=0} \qquad (6)$$

$$\begin{cases} \int_{-d}^{0} \psi_{3,n}\phi_3 dz = \int_{-d}^{0} \psi_{3,n}\phi_2 dz \\ \int_{-h_3}^{0} \psi_{3,n}\partial\phi_3/\partial x dz = \int_{-d}^{0} \psi_{3,n}\partial\phi_2/\partial x dz \end{cases}, \quad \text{for x=L} \qquad (7)$$

Case 2, porous bar:

$$\begin{cases} \int_{-h_1}^{0} \psi_{1,n}\phi_1 dz = \int_{-h_2}^{-d} \psi_{1,n}\phi_{2\,\mathrm{inf}}\, dz + \int_{-d}^{0} \psi_{1,n}\phi_{2\,\mathrm{sup}}\, dz \\ \int_{-h_1}^{0} \psi_{1,n}\partial\phi_1/\partial x dz = \int_{-h_2}^{d} \psi_{1,n}\partial\phi_{2\,\mathrm{inf}}/\partial x dz + \int_{-d}^{0} \psi_{1,n}\partial\phi_{2\,\mathrm{sup}}/\partial x dz \end{cases}, \quad \text{for x=0} \quad (8)$$

$$\begin{cases} \int_{-h_1}^{0} \psi_{3,n}\phi_3 dz = \int_{-h_2}^{-d} \psi_{3,n}\phi_{2\,\mathrm{inf}}\, dz + \int_{-d}^{0} \psi_{3,n}\phi_{2\,\mathrm{sup}}\, dz \\ \int_{-h_3}^{0} \psi_{3,n}\partial\phi_3/\partial x dz = \int_{-h_2}^{d} \psi_{3,n}\partial\phi_{2\,\mathrm{inf}}/\partial x dz + \int_{-d}^{0} \psi_{3,n}\partial\phi_{2\,\mathrm{sup}}/\partial x dz \end{cases}, \quad \text{for x=L} \quad (9)$$

Case 3, porous bar with impervious walls:

$$\begin{cases} \int_{-d}^{0} \psi_{1,n}\phi_1 dz = \int_{-d}^{0} \psi_{1,n}\phi_{2\,\mathrm{sup}}\, dz \\ \int_{-h_1}^{0} \psi_{1,n}\partial\phi_1/\partial x dz = \int_{-h_2}^{d} \psi_{1,n}\partial\phi_{2\,\mathrm{inf}}/\partial x dz + \int_{-d}^{0} \psi_{1,n}\partial\phi_{2\,\mathrm{sup}}/\partial x dz \end{cases}, \quad \text{for x=0} \quad (10)$$

$$\begin{cases} \int_{-h_1}^{0} \psi_{3,n}\phi_3 dz = \int_{-d}^{0} \psi_{3,n}\phi_{2\,\mathrm{sup}}\, dz \\ \int_{-h_3}^{0} \psi_{3,n}\partial\phi_3/\partial x dz = \int_{-h_2}^{d} \psi_{3,n}\partial\phi_{2\,\mathrm{inf}}/\partial x dz + \int_{-d}^{0} \psi_{3,n}\partial\phi_{2\,\mathrm{sup}}/\partial x dz \end{cases}, \quad \text{for x=L} \quad (11)$$

The reflection coefficient is then given by

$$R = \left| \frac{A_{1,0}^{+}}{A_{1,0}^{-}} \right| \tag{12}$$

4. Results

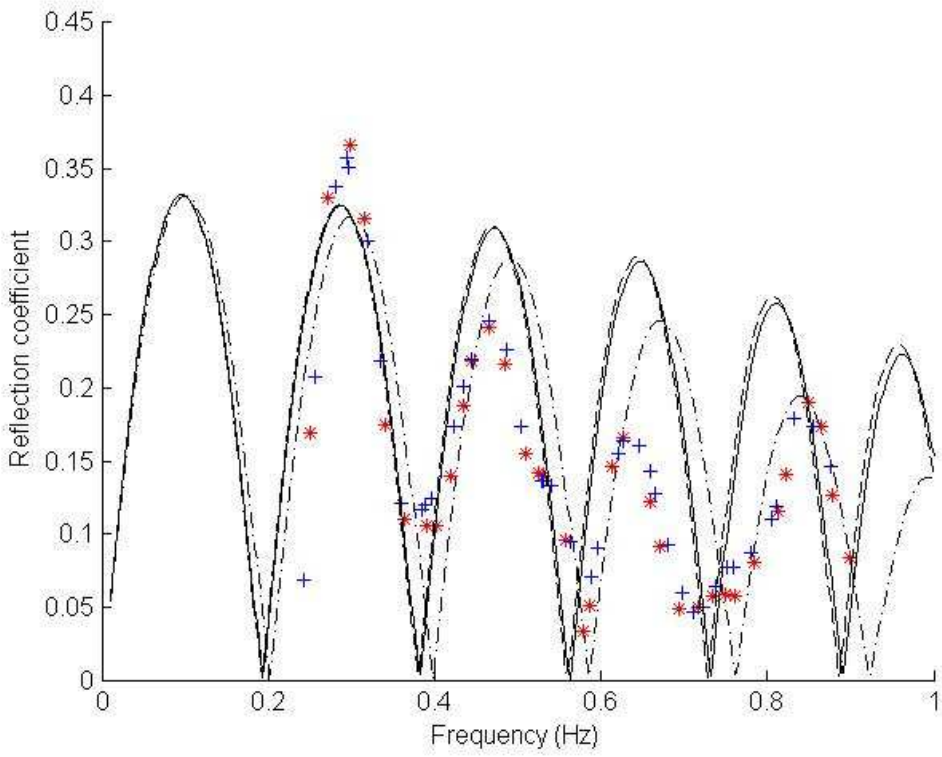

Figure 2. Wave reflection versus frequency, impervious bar; Model : P = 0 (- · -), P = 1 (—), P = 10 (- - -), Experiments:(*) Series 1a, (+) Wave amplitudes, Series 1b

4.1 Wave reflection

Results concerning the wave reflection for series 1 are presented in Figs. 2 and 3 for respectively the impermeable and the porous beds. They are compared to numerical calculations based on the integral matching methods for both solid and porous bars. It is already known that the peaks and minima of reflection are shifted by the presence of the evanescent modes, which are then taken into account in the calculations. For the porous case, the solutions corresponding to evanescent modes are no more only evanescent but include a propagating term due to the more complex dispersion relation (Yu and Chwang, 1994). In the present calculation, a dissipative behavior of the wave induced motion through the porous media is assumed for the solution of the dispersion relation. We can observe that taking into account the presence of the evanescent modes only acts on the amplitude of the reflection but do not affect the location of the minima. This is understandable since the adaptation of the wave at the step is smoothed by the permeability of the porous bar. The experimental results (see Figs. 2 and

3) follow the oscillating behavior of the reflection coefficient, for both series 1a and 1b.

In addition, the locations of the minima observed for the solid bar seem not to be significantly shifted for the porous case.

For the second series of experiments, only a porous bed was considered, but either solid or porous vertical boundaries were tested. Results are given in Fig. 4. We can observe that the solid vertical boundaries do not have any influence on the reflection process. These results tend to demonstrate that the interference process above the bar is not sensitive to the edge dynamics.

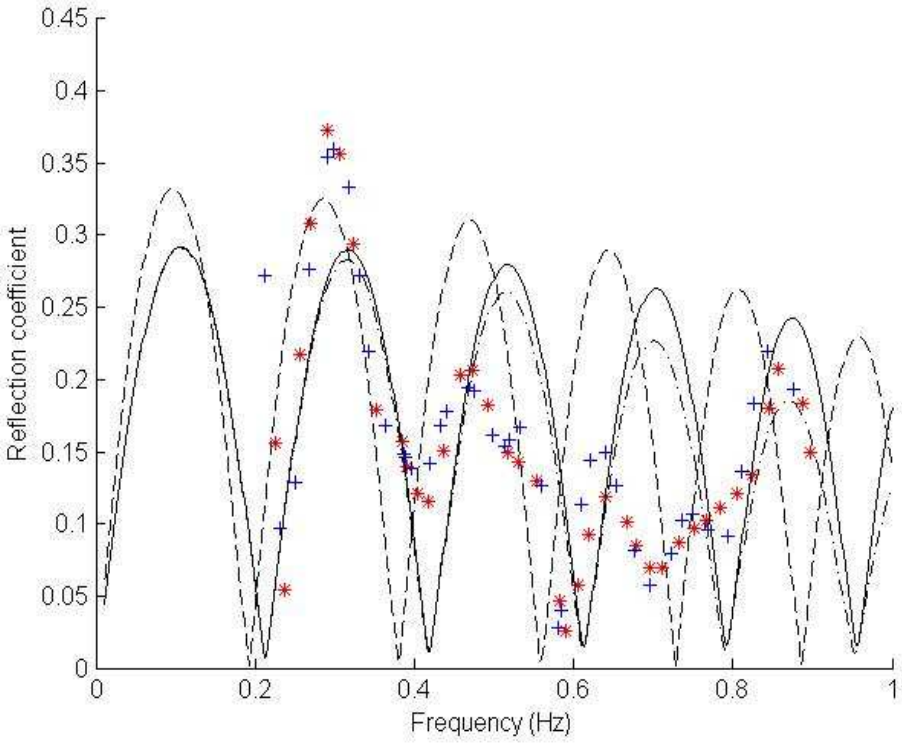

Figure 3. Wave reflection versus frequency,porous bar, Model :impervious bar, P = 10 (- - -), porous bar,, P = 0 (- · -), P = 1 (—); Experiments:(*) Series 1a, (+)Series 1b

4.2 Wave phase evolution over the bar

Since the far field effect (reflection coefficient) of the interference process above the bar seemed not to depend on the porosity of the studied porous bed, wave phase along the bar was measured through synchronized gauges. The averaged (over a distance of 1.5m) wave crest celerity above the obstacle is presented in Fig. 5 for f=0.58Hz.

We can observe that the celerity is higher for the porous bed for the more up-wave positions. It is the higher of about 7% for X=0.75 (averaged celerity between X=0 and X=1.5m). This may be ascribed to an “entrance length”, since the dynamics within the porous is not only forced by the above wave induced pressures but also to the wave forcing at the vertical step. However, we also can observe that the wave celerity remains higher than the theoretical value assuming a linear progressive

wave above a flat bed. This behavior may be due to the fact that the wave celerity is calculated through the celerity of the crest, which does not only depend to the incoming progressive wave but also on the presence of the reflected wave, of the evanescent modes. The harmonic effects are discarded by use of a Fourier analysis of the signal.

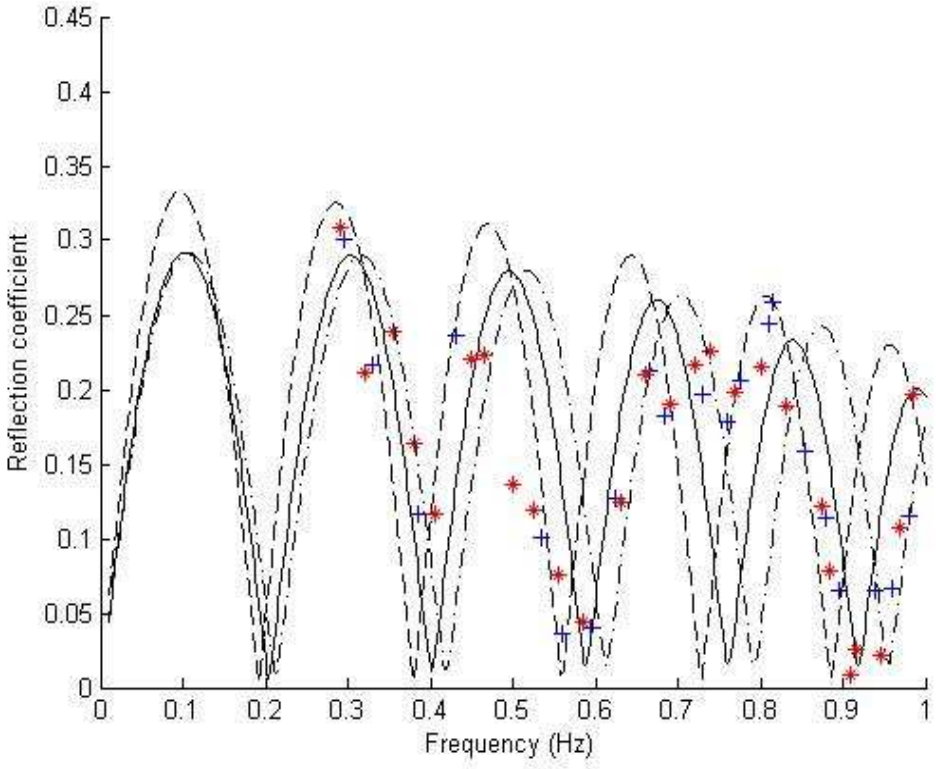

Figure 4. Wave reflection versus frequency; Model : impervious bar, P = 10 (- - -), porous bar, P = 1 (- · -), porous bar with impervious walls, P = 1 (—); Experiments:(*) porous walls, (+) impervious wall

4.3 Wave induced motion in the vicinity of the bar

In order to better understand the impact of the steps on the dynamics, the velocity was measured near the steps on both sides of the porous bar, for either impervious or porous vertical boundaries. Both horizontal and vertical velocities are presented in Fig. 6 for X=-3cm and Z=1, 8.5 and 16cm. Four wave amplitudes are considered, the frequency f= Hz is fixed.

We can observe discrepancies for the horizontal component near the bed, which can be easily explained by the porous wall in one case which allows a mass flux across the vertical boundary. Both the vertical velocities and the horizontal velocity just above the level of the bar give similar results. In addition we can observe a linear behavior of the velocity increase with increasing wave amplitude.

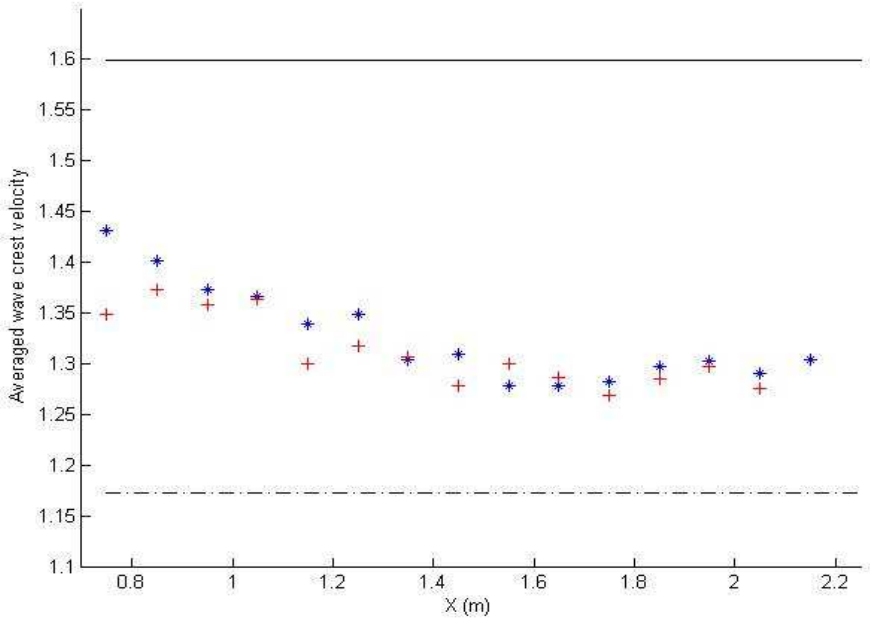

Figure 5. Averaged wave crest velocity versus X-axis, Experiments: (+) impermeable obstacle, (*) porous obstacle, (- - -) wave celerity, h=0.15 m, (—) wave celerity, h=0.30 m

5. Discussion and conclusion

In the present study, the wave propagation over a rectangular porous bar was investigated. The measurements of the reflection coefficient versus frequency for both porous and impervious bars were first compared to numerical results based on linear theories for gravity waves. The results have shown that the interference process, which is seen through the oscillating behavior of the reflection coefficient versus frequency, is weakly influenced by the porosity of the bar. The use of impervious vertical boundaries at both sides of the bar has no more effects on the reflection coefficient. In order to confirm this result through the local wave properties, the wave celerity was measured along the bar location. A slight difference was observed at the up-wave step, which rapidly disappeared along the bar. Velocity measurements near this vertical step showed a linear increase of both horizontal and vertical velocity components. In the case of an impervious vertical wall, a significant difference is observed for the horizontal velocity component, especially at the foot of the step, what is in accordance with the impermeable condition in this latter case. However, the step effects on both the velocity field and the celerity due to either porous or permeable bar conditions remain a local effect since it has no global influence on the interference process as observed for the analysis of the reflection coefficient. The absence of such local effects on the far field wave behavior has been already observed in the case of solid rectangular bar in terms of local turbulence associated with the generation of vortices at the corners of the bar (Rey et al, 1992).

However, in the present case, the porous media enhances dissipation due to both its roughness and

the flow induced within the porous bed. Analysis of wave damping above the bar including non-linear effects is in progress. One of the goals is the characterization of the porous through analysis of both the wave celerity and damping.

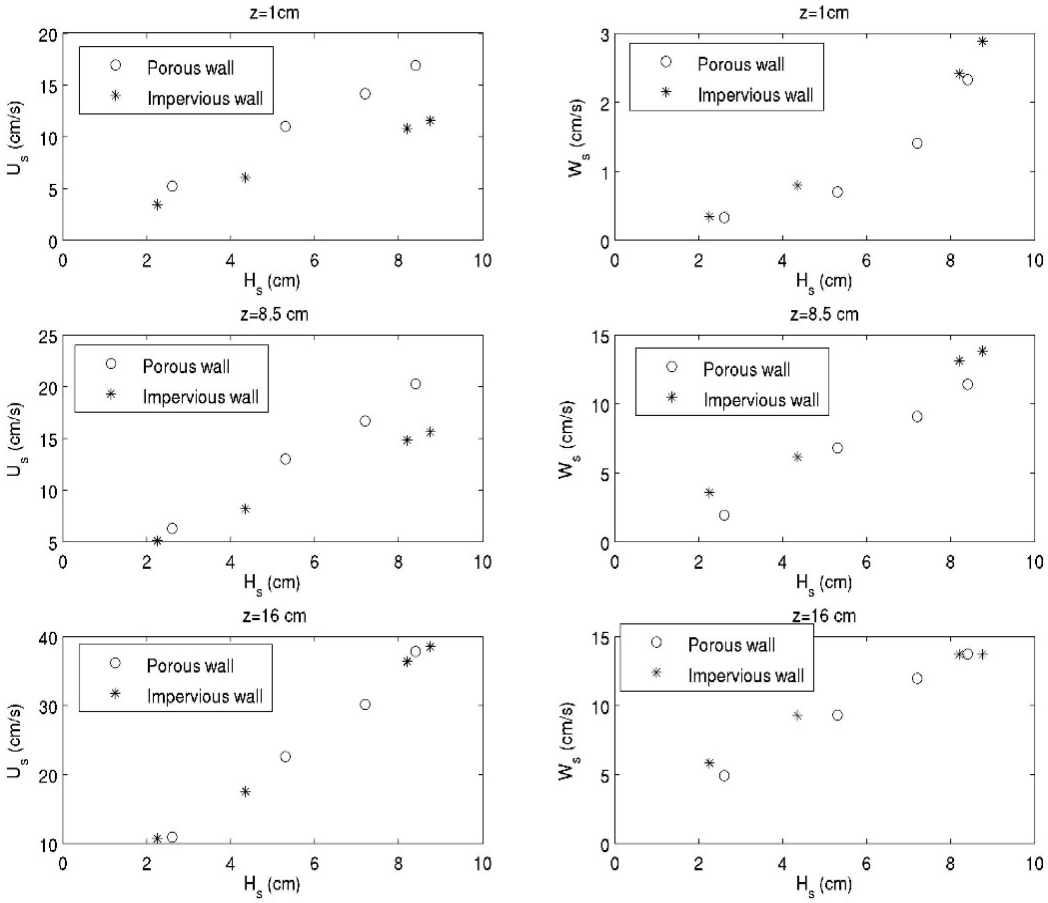

Figure 6. Horizontal (left) and vertical (right) velocities versus wave height for Z=1cm (up), Z=8.5 cm (middle) and Z=16cm (bottom)

References

Guazzelli, E., Rey, V., and Belzons, M. 1992. Higher-order Bragg reflection of gravity surface waves by periodic beds, *J. Fluid Mech*,. 245:, 301-317.

Liu, P. L. F. and Dalrymple, R. A. 1984. The damping of gravity water-waves due to percolation. *Coastal. Eng*. 8: 33-49.

Magne, R., Belibassakis, K. A., Herbers, T. H. C., O'Reilly, W. C., Ardhuin, F. and Rey, V. (2007). Evolution of surface gravity waves over a submarine canyon, *J. Geophys. Res.*, 112, C01002.

Rey, V. 1992. Propagation and local behaviour of normally incident gravity waves over varying topography, *European Journal of Mechanics B/Fluids*, 11: 213-232.

Rey, V., Belzons, M. and Guazzelli, E. 1992. Propagation of surface gravity waves over a rectangular submerged bar, *J. Fluid Mech,*. 235: 453-479.

Yu, X.and Chwang, A. T. 1994. Wave motion through porous structures. *J. Eng. Mech.* 120: 889-1008.